We are IntechOpen, the world's leading publisher of Open Access books Built by scientists, for scientists

4,800
Open access books available

122,000
International authors and editors

135M
Downloads

Our authors are among the

154
Countries delivered to

TOP 1%
most cited scientists

12.2%
Contributors from top 500 universities

CLARIVATE ANALYTICS BOOK CITATION INDEX INDEXED

WEB OF SCIENCE™

Selection of our books indexed in the Book Citation Index in Web of Science™ Core Collection (BKCI)

Interested in publishing with us?
Contact book.department@intechopen.com

Numbers displayed above are based on latest data collected.
For more information visit www.intechopen.com

1

MOZ-TIF2 Fusion Protein Binds to Histone Chaperon Proteins CAF-1A and ASF1B Through Its MOZ Portion

Hong Yin[1], Jonathan Glass[1] and Kerry L. Blanchard[2]
[1]*Department of Medicine and the Feist-Weiller Cancer Center, LSU Health Sciences Center, Shreveport, LA*
[2]*Eli Lilly & Company, Indianapolis, IN*
USA

1. Introduction

We previously identified a MOZ-TIF2 (transcriptional intermediary factor 2) fusion gene from a young female patient with acute myeloid leukemia (AML) (Liang et al., 1998). MOZ related chromosome translocations include MOZ-CREB-binding protein (MOZ-CBP, t(8;16)(p11;p13)), MOZ-P300(t(8;22)(p11;q13)), MOZ-TIF2(inv(8)(p11q13), and MOZ-NCOA3(t(8;20)(p11;q13)) (Esteyries et al., 2008; Troke et al., 2006). In an animal model, the MOZ-TIF2 fusion product successfully induced the occurrence of AML (Deguchi et al., 2003). Though the mechanisms for leukemogenesis of this fusion protein are poorly understood, analysis of functional domains in the MOZ-TIF2 fusion protein discloses at least two distinct functional domains: 1) the MYST domain containing the C2HC nucleosome recognition motif and the histone acetyltransferase motif in the MOZ portion and 2) the CID domain containing two CBP binding motifs in the TIF2 portion. Together these domains were responsible for AML in mice caused by injecting bone marrow cells transduced with retrovirus containing the MOZ-TIF2 fusion gene. Furthermore, MOZ-TIF2 conferred the properties of leukemic stem cells (Huntly et al., 2004). The MOZ-TIF2 transduced mouse common myeloid progenitors and granulocyte-monocyte progenitors exhibited the ability to serially replated *in vitro*. The cell line derived from transduced progenitors could induce AML in mice. Interestingly, the C543G mutation in C2HC nucleosome recognition motif or in the CBP binding motif (LXXLL) blocked the self-renewal function of MOZ-TIF2 transduced progenitors. More recently, a study using PU.1 deficient mice demonstrated that the interaction between MOZ-TIF2 and PU.1 promoted the expression of macrophage colony–stimulating factor receptor (CSF1R). Cells with high expression of CSF1R are potential leukemia initiating cells(Aikawa et al., 2010). Models suggesting that aberrant transcription by the interaction between MOZ fusion proteins and transcription factors, AML1, p53, PU1, or NF-kB have been well reviewed(Katsumoto et al., 2008).

MOZ as a fusion partner of MOZ-TIF2 is a member of MYST domain family (MOZ/YBF2/SAS2/TIP60) and acetylates histones H2A, H3 and H4 as a histone acetyltransferase (HAT) (Champagne et al., 2001; Kitabayashi et al., 2001). MOZ is a cofactor

in the regulation of transcriptional activation of several target genes important to hematopoiesis, such as Runx1 and PU.1 (Bristow and Shore, 2003; Katsumoto et al., 2006; Kitabayashi et al., 2001). MOZ$^{-/-}$ mice died at embryonic day 15 and exhibited a significant decrease of mature erythrocytes (Katsumoto et al., 2006). The histone acetyltransferase activity of MOZ is required to maintain normal functions of hematopoietic stem cells (HSC) (Perez-Campo et al., 2009). Mice with mutation at HAT or MYST domain (G657E) showed a decreased population of HSC in fetal liver. The lineage-committed hematopoietic progenitors from fetal liver cells with HAT$^{-/-}$ mutant had reduced colony formation ability.

In our attempt to find proteins that interact with the fusion protein by using as bait a construct of the MOZ N-terminal fragment, encoding the first 759 amino acids of MOZ-TIF2 fusion gene and containing the H15, PHD, and MYST domains, we were able to isolate two proteins, the p150 subunit or subunit A of the human chromatin assembly factor-1 (p150/CAF-1A) and the human anti-silencing function protein 1 homolog B (ASF1B). Both of these proteins were verified to interact with the MOZ partner of MOZ-TIF2 fusion in the yeast two-hybrid system. The interaction has been further characterized by co-immunoprecipitation, protein pull-down assays, and co-localization by immunohistochemistry. The differences in the interactions of CAF-1A and ASF1B with wild type MOZ and the MOZ-TIF2 fusion proteins may contribute to leukemogenesis.

2.Materials and methods

2.1 The sources of cDNAs and plasmid constructions

The cDNA for MOZ was kindly provided by Julian Borrow (Center for Cancer Research, Massachusetts Institute of Technology, MA) and TIF2 was a kind gift from Hinrich Gronemeyer (Institut de Genetique et de Biologie Moleculaire et Cellulaire, France). A full length MOZ-TIF2 fusion was created by inserting a RT-PCR fragment crossing the MOZ–TIF2 fusion site into the Hind3 site of wild type of human MOZ and the Sac1 site of human TIF2 in pBluescript KS phagemid vector (pBlueKS). The cDNAs for CAF-1A and ASF1B were screened and rescued from Human Bone Marrow MATCHMAKER cDNA Library (BD Biosciences Clontech Palo Alto, CA) by the yeast two-hybrid system using the N-terminal fragment of the MOZ-TIF2 fusion as bait. The cDNAs from the positive clones, which were in the pACT2 vector, were switched into the pBlueKS vector at EcoRI and XhoI sites and sequenced with a T7 primer. The resulting sequences were identified in the NCBI GenBank as the subunit A (p150) of human chromatin assembly factor-1 (GenBank accession No. NM-005483) and human anti-silencing function protein 1 homolog B (GenBank accession No. AF279307). The full length of both cDNAs was confirmed by DNA sequencing with gene specific primers. For the visualization of the expression and localization in mammalian cells, the full length of MOZ, MOZ-TIF2, TIF2, CAF-1A, and ASF1B were subcloned in frame into the C-terminal fluorescent protein Vector, pEGFP or pDsRed2 (BD Biosciences Clontech, Palo Alto, CA) to generate fluorescent fusion proteins. For studies of protein-protein interaction *in vitro*, glutathione S-transferase (GST) fusions of MOZ fragments were constructed in the pGEX vector (Amersham Biosciences, Piscataway, NJ). Briefly, the full length MOZ cDNA was digested with Asp718/BgI2 from pBlueKS-MOZ and was ligated into the pET-30a (EMD Biosciences, Inc. Novagen Madison, WI) plasmid at Asp718/BamH1 site to create the pET-30a-MOZ construct. A PET-30a-MOZ-1/759 (amino acids 1 to 759)

construct was generated by removing a Hind3/Hind3 fragment from pET-30a-MOZ and then re-ligating. This fragment was then switched from pET-30a vector to pGEX-4T at a Not1/Xho1 site to construct the pGEX-4T-MOZ-1/759. The pGEX-4T-MOZ-1/313 (amino acids 1 to 313) containing H15 and the PHD domain was generated by the deletion of a 1515 base pair fragment from pGEX-4T-MOZ-1/759 with Hind3 /Blin1 followed by re-ligation. The pGEX-6P-MOZ-488/703 plasmid was constructed by inserting an EcoRV to Eag1 fragment of MOZ (amino acids 488 to 703) containing the C2HC motif and acetyl-CoA binding region to pGEX-6P-2 vector at Sma1/Eag1 sites. To create pET-30a-CAF-1A, the pBlueKS-CAF-1A was first digested with XhoI and then digested partially with NcoI. A 3.1 kb fragment was recovered by agarose electrophoresis and was ligated to NcoI/XhoI sites of pET-30a vector. The pET-30c-ASF1B was constructed by inserting the 1 kilobase EcoR1/Hind3 fragment of pBLueKS-ASF1B into the pET-30c vector at EcoR1 /Hind3 sites.

2.2 Yeast two-hybrid screen

pGBD-MOZ-MYST, a bait plasmid with a fusion of the N-terminal fragment of MOZ-TIF2 to the GAL4 DNA binding domain was constructed by inserting a 2.3 kb fragment encoding amino acids 1 to 759 of human MOZ to BamH1/blunted Bgl 2 sites in the pGBD-C3 vector (James et al., 1996). The bait plasmid was transformed into the yeast host PJ69-2A and mated with pre-transformed Human Bone Marrow MATCHMAKER cDNA Library according to the manufacturer's instruction. The mating culture was plated on 25 x 150 mm triple dropout (TDO) dishes (SD/-His/-Leu/-Trp) and 25 x 150 mm quadruple dropout (QDO) dishes (SD/-Ade/-His/-Leu/-Trp). After incubation for 7 and 14 days, the more than 100 colonies which grew on TDO and QDO dishes were picked for re-screening on SD/-His, SD/-Ade/ and QDO dishes. A total of five colonies were grown from the second screening. The plasmids from each colony were rescued and transformed into KC8 cells. All of the plasmids were re-transformed into the yeast host PJ69-2A and Y187; no auto-transcription activation of any reporter was seen. The pVA3.1 plasmids containing either the murine p53 in PJ69-2A or the PTD1-1 with SV 40 large T antigen in Y187 were used as controls for DNA binding domain and activation domain fusions. The plasmids from positive clones were subjected to restriction enzyme mapping which showed two potential interacting genes which were subsequently sequenced and identified with the NCBI database.

2.3 Co-localization of MOZ or MOZ-TIF2 and CAF-1A or ASF1B

To identify the co-localization of expressed fluorescent fusion proteins, HEK293 cells were grown in DMEM (Mediatech Cellgro, VA) containing 10% fetal bovine serum (FBS) and co-transfected by pEGFP-MOZ or pEGFP-MOZ-TIF2 and pDsRed2-CAF-1A or pDsRed2-ASF1B with Lipofectamine 2000 (Invitrogen, Carlsbad, CA). Briefly, cells were grown on a coverslip in a 12-well plate a day before the transfection in the antibiotic-free medium to reach 80-90% confluence on the next day. 1.6 μg of DNA in 100 μl of Opti-MEM I Reduced Serum Medium (Invitrogen, Carlsbad, CA) was mixed with 100 μl of diluted Lipofectamine 2000 reagent. After incubation for 20 min. at room temperature, the DNA-Lipofectamine 2000 complex was added to the cells and 48 hours later, subcellular location of expressed fluorescent fusion proteins was examined with a Zeiss fluorescent microscope equipped with Axiocam system and by a laser scanning confocal microscope (Bio-Rad Laser Scanning

System Radiance 2000/Nikon Eclipse TE300 microscope). To examine the subcellelular localization of endogenously expressed MOZ and CAF-1A, HEK293 and Hela cells were fixed with 4% paraformaldehyde and then blocked with Ultra V block (Lab Vision Co.CA). For some experiments pre-extraction with 0.3%Triton-X100 was conducted. The fixed cells were then incubated with antibody against MOZ (N-19, Santa Cruz Biotechnology, Inc, Santa Cruz, CA) at 1:100 and /or antibody against CAF-1A (a kind gift from Dr. Bruce Stillman, Cold Spring Harbor, NY). In some experiments, the antibody against CAF-1A and ASF1B were purchased from Cell Signaling Technology, MA. The immunofluorescence of MOZ, CAF-1A, or ASF1B was observed as described above for examination of expressed EGFP fusion proteins.

2.4 Co-immunoprecipitation and immunoblotting

HEK293 cells were transfected with EGFP fusions of MOZ, MOZ-TIF2, or TIF2. After 48 hours of transfection, whole cell lysates was prepared with plastic individual homogenizers in the lysis buffer [50 mM NaCL, 5mM KCL, 1mM EDTA, 20 mM HEPES, pH 7.6, 10% glycerol, 0.5% NP-40, and protease inhibitor cocktails (Roche Applied Science, IN)]. Immunoprecipitation was conducted with an antibody against EGFP (BD Biosciences, Palo Alto, CA). Briefly, 2 μg of anti-EGFP antibody and protein A/G-agarose (Santa Cruz Biotechnology, Santa Cruz, CA) were added to 0.8 ml of cell lysate (about 500 μg protein) and incubated overnight at 4°C with rotation. The precipitate was collected by centrifugation, extensively washed, subjected to SDS-PAGE, transferred onto Hybond-ECL nitrocellulose membrane (Amersham Pharmacia Biotech, Piscataway, NJ), and examined by immunoblotting with the antibody against CAF-1A.

2.5 Expression of GST fusion proteins and GST pull down assay

E. *coli* BL21-CodonPlus®(DE3)-RIL Competent Cells (Stratagene, La Jolla, CA) were transformed with pGEX vectors containing cDNA fragments MOZ-1/759, MOZ-1/313, or MOZ-488/703 and grown in LB medium. To induce protein expression isopropyl β-D-thiogalactopyranoside (IPTG) was added at final concentration of 1mM when the A_{600} of the cultures reached 0.6 to 0.8. After three more hours of growth at 28° C, cells were collected by centrifugation and resuspended in cold PBS containing 1% Triton X-100 and protease inhibitor cocktail and kept on ice for 30 minutes. Cell lysates were prepared by ultrasonication followed by centrifugation at 15,000 rpm for 30 minutes at 4˚C. GST fusion proteins were purified with the GST Purification Module (Amersham Pharmacia Biotech, Piscataway, NJ). Purified GST fusion proteins were examined with SDS-PAGE followed by Coomassie Blue staining. To perform GST pull down affinity assays [^{35}S]Methionine-labeled proteins were first produced with Single Tube Protein® System 3 or EcoPro™ T7 system (EMD Biosciences, Inc. Novagen, Madison, WI) from pET 30 vectors carrying full length of CAF-1A or ASF1B. The binding reaction was conducted with 5μl of *in vitro*-translated protein and 3-5 μg of GST alone or GST fusion protein attached to Sepharose 4B beads in 200 μl binding buffer (50mM Tris-HCI , pH 8.0, 100 mM NaCl, 0.3 mM DTT, 10mM MgCl2, 10% glycerol, 0.1% NP40). The reaction was conducted at 4 °C for 1 hour followed by five washes with 400 μl of binding buffer. The final pellet was separated by SDS-PAGE, autoradiography performed, and radioactivity detected with a phosphorimager.

2.6 *In Vitro* protein binding assay with S-tagged fusion protein

The S-tagged fusion of ASF1B was expressed from pET-30c-ASF1B in E. *coli* BL21-CodonPlus® (DE3)-RIL cells after induction with 0.8 mM of IPTG and purification with S-tagged agarose beads. The fusion protein on agarose beads was incubated with 150µl (about 600 µg of protein) of cell extract from HEK293 cells transfected with pEGFP fusion protein. The beads were pelleted, washed, and the "pull-down" proteins examined as described above with the anti-EGFP antibody.

2.7 RNA isolation and microarray analysis

RNA was isolated from stably transfected U937 cells with TRI Reagent® (Molecular Research Center, Inc., Cincinati, OH). The analysis of gene expression profile was conducted on the Human Genome U95A Array (Affymetrix, Inc., Santa Clara, CA). The cRNA was synthesized from 10µg of total RNA. The hybridization and signal detection was completed in the Core Facility at LSUHSC-Shreveport according to the standard Affymetrix protocol. The human U95A array represents 12,256 oligonucleotides of known genes or expression tags. The expression profile was analyzed with GeneSifter software. In pairwise analysis, the quality was set as 0.5 for at least one group in order to minimize the effect of low intensity or poor quality spots. Genes with a $\geq$ 2-fold change and with $P<0.05$ in a student T-test were considered as either significantly up or down regulated genes. To find genes either commonly or differentially expressed in the gene list, we set the quality as 1 to obtain positive expressed genes in pattern navigation analysis. The analysis results were exported for Venn Diagram analysis using the GeneSifter intersector tool.

3.Results

3.1 Screening for MOZ interacting proteins by the yeast two-hybrid system

A MOZ cDNA fragment encoding amino acids 1 to 759 cloned into pGBD was used as the bait in the yeast two-hybrid system in which the prey was a human cDNA bone marrow library. After a second screening five β-galactosidase positive clones grew on SD/-His plates. To eliminate any of these clones as representing false positive clones, plasmid DNA from each clone was rescued using KC8 cells and transformed into PJ69-2A cells carrying pGDB-MOZ-MYST. The transformants were then selected on five different media: –Trp/ -Leu, -His, -His+5mM 3-amino-1,2,4-triazole (3-AT), -His+10mM 3-AT, and –Ade and interaction with the MOZ fragment was verified in all five of the clones (Figure 1). Clone 3.1 grew on –His, -His+10mM 3-AT, and –Ade medium indicative of a strong physical interaction; the other clones only grew on –His and –His + 5 mM 3-AT, but not on –Ade, indicating a weaker interaction. DNA sequencing of the putatively strongly MOZ interacting protein demonstrated that the cDNA encoded the full length CAF-1A. The more weakly interacting cDNAs represented the entire coding region of ASF1B.

3.2 Identify the interaction between MOZ and CAF-1A in human cells

In yeast, the MYST family member Sas2 was found to interact with Cac1, the largest subunit of Saccharomyces cerevisiae chromatin assembly factor-I (CAF-1) (Meijsing and Ehrenhofer-Murray, 2001) but it is not known if the interaction between the homologous proteins in

mammalian cells, MOZ and CAF-1A, takes place in human cells and if any interaction occurs between the MOZ-TIF2 fusion protein and CAF-1A. To address these areas we looked for interactions by co-immunoprecipitation using transfections with the

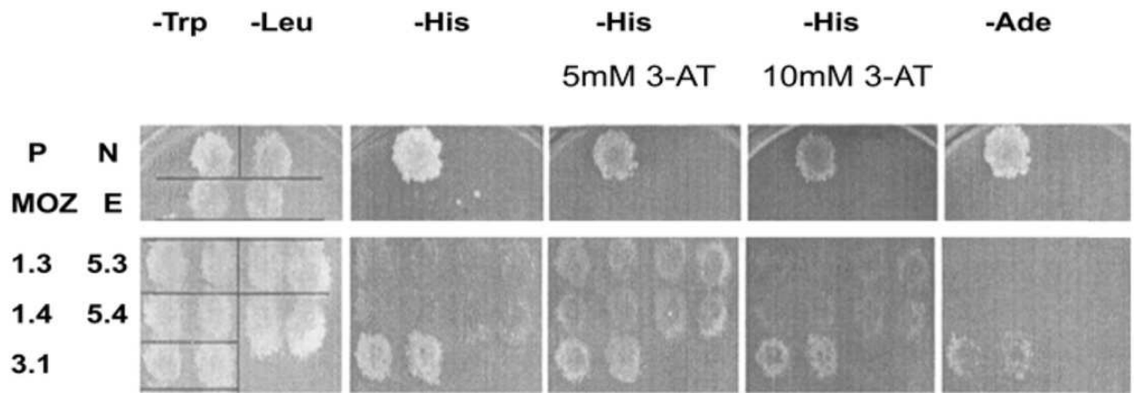

Fig. 1. Protein interaction between MOZ and CAF-1A or ASF1B in the yeast two-hybrid system. The yeast two-hybrid system was used with pretransformed Matchmaker libraries as detailed in the Methods. The bait was the fragment encoding amino acids 1 to 759 of the human MOZ gene in the pGAL 4 DNA-BD vector. In the upper panel controls are plated on 5 different selection media: **P**, positive control diploid with plasmid pDT1-1 encoding an AD/SV40 large T-antigen fusion protein and pVA3-1 carrying DNA-BD/murine P53 fusion protein. **N**, negative control diploid. MOZ, a diploid with GAL4 DNA-BD+ MOZ fragment of amino acids 1 to 759. **E**, a diploid with GAL4 DNA-BD vector only. In the lower panel the five clones (1.3, 1.4, 3.1, 5.3, and 5.4) that were positive after a second screening were plated in duplicate on the same media. Clones 1.3, 1.4, 5.3, and 5.4 show an interaction between MOZ and ASF1B; clone 3.1 shows an interaction between the MOZ and CAF-1A. Trp, tryptophan, Leu, leucine, His, histidine, Ade, adenine, 3-AT, 3-amino-1,2,4,triazole.

MOZ and MOZ-TIF2 fusion constructs into HEK293 cells which express CAF-1A (Figure 2). In these experiments the HEK293 cells were transfected with EGFP fusions of MOZ, MOZ-TIF2 and TIF2, the expressed fusion proteins precipitated with anti-EGFP antibody and the presence of co-precipitated CAF-1A assayed by western blot analysis. Only with the product of the EGFP-MOZ construct was a significant amount of CAF-1A precipitated (Figure 2A); a far smaller amount was precipitated with MOZ-TIF2. By comparison to the intensity of the CAF-1A band in the input lane, which represents 10% of the amount of lysate subjected to immunoprecipitation, approximately 35-40% of the HEK293 cell CAF-1A was estimated to be co-precipitated with the transfected MOZ. In contrast, less than 10% of the CAF-1A co-precipitated with MOZ-TIF2 (Figure 2A). The differences in the amount of CAF-1A precipitated were not a result of altered expression of CAF-1A or of differences in expression levels of the transfectants as the expression of CAF-1A was not affected by any of the three transfectants (Figure 2B) and the EGFP-tagged MOZ and MOZ-TIF2 proteins showed similar levels of expression, while TIF2 showed a 2-3 fold higher expression than MOZ and MOZ-TIF2 (Figure 2C).

3.3 The MOZ portion of MOZ-TIF2 fusion interacts physically with CAF-1A through the N-terminal of MOZ

Using the yeast two-hybrid system we have shown that CAF-1A interacted with a MOZ fragment extending from amino acids 1 to 759. Within this region are PHD (amino acids 195-320) and MYST (amino acids 562-750) domains that are potential sites for the interaction with (Figure 3A) (Champagne et al., 1999).

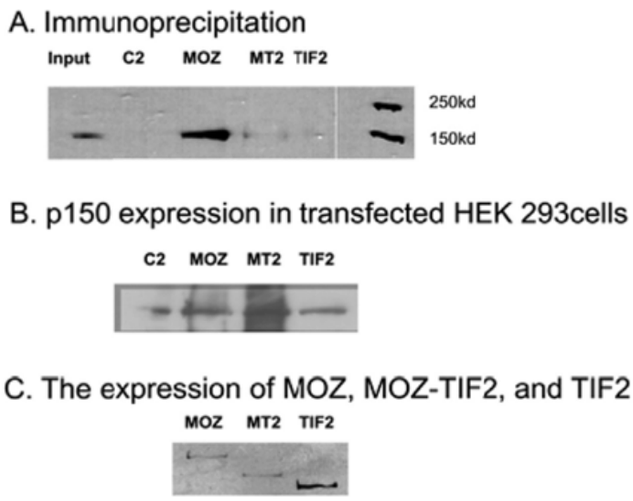

Fig. 2. **Co-precipitation of CAF-1A (p150) with EGFP-tagged MOZ, MOZ-TIF2, and TIF2.** The EGFP constructs of MOZ, MOZ-TIF2, and TIF2 were transfected into HEK293 cells. **Panel A.** After 48 hours, whole cell extracts were prepared in lysis buffer and subjected to immunoprecipitation with anti-EGFP antibody, followed by SDS-PAGE, and western blot analysis with anti-p150 antibodies. The input lane corresponds to 10% of the amount of lysate subjected to immunoprecipitation. Lane C2 represents the pEGFP-C2 vector alone and MT2 represents MOZ-TIF2. **Panel B**. The lysates of the various transfectants were subjected to SDS-PAGE followed by western blot analysis with anti- p150 antibody to demonstrate the expression level of p150 in the transfected cells. **Panel C**. The same lysates used in Panel B were subjected to a western blot analysis with anti-EGFP antibody to demonstrate the expression of EGFP-tagged MOZ, MOZ-TIF2 and TIF2.

To further define the region containing the binding domain, a pull down assay using GST fusion proteins was established. First, a GST-tagged MOZ fragment from amino acids 1 to 759 was used to pull down CAF-1A and to demonstrate that the GST did not interfere with the MOZ-CAF-1A interactions shown earlier (Figure 3B). We then generated two GST-tagged MOZ fragments, one encompassing amino acids 1-313 (MOZ-1/313) containing the H15 and PHD domains and the other from amino acids 488-703 (MOZ-488/703) including the C2HC motif and acetyl-CoA binding region (Figure 3 C, left panel). These peptides were used with [^{35}S]methionine labeled CAF-1A synthesized in an *in vitro* translation system and interactions detected with a GST pull down assay (Figure 3C). For equivalent amounts of fusion peptides more MOZ-1/313 was bound to CAF-1A than MOZ-488/703 (Figure 3C). As a percentage of the input radioactivity, MOZ-1/313 pulled down about 30 % of the [^{35}S]methionine labeled CAF-1A while MOZ-488/703 pulled down only 14%. Further

analysis of domain interactions showed that strongest binding was seen between MOZ-1/313 and CAF-1A-176/327 among all peptides (Figure 3D). CAF-1A-176/327 pulled down about 328% of [35S]methionine labeled MOZ-1/313 and pulled down only 76% of MOZ-488/703 while CAF-1A-620/938 pulled down 20% and 28% of MOZ-1/313 and MOZ-488/703, respectively.

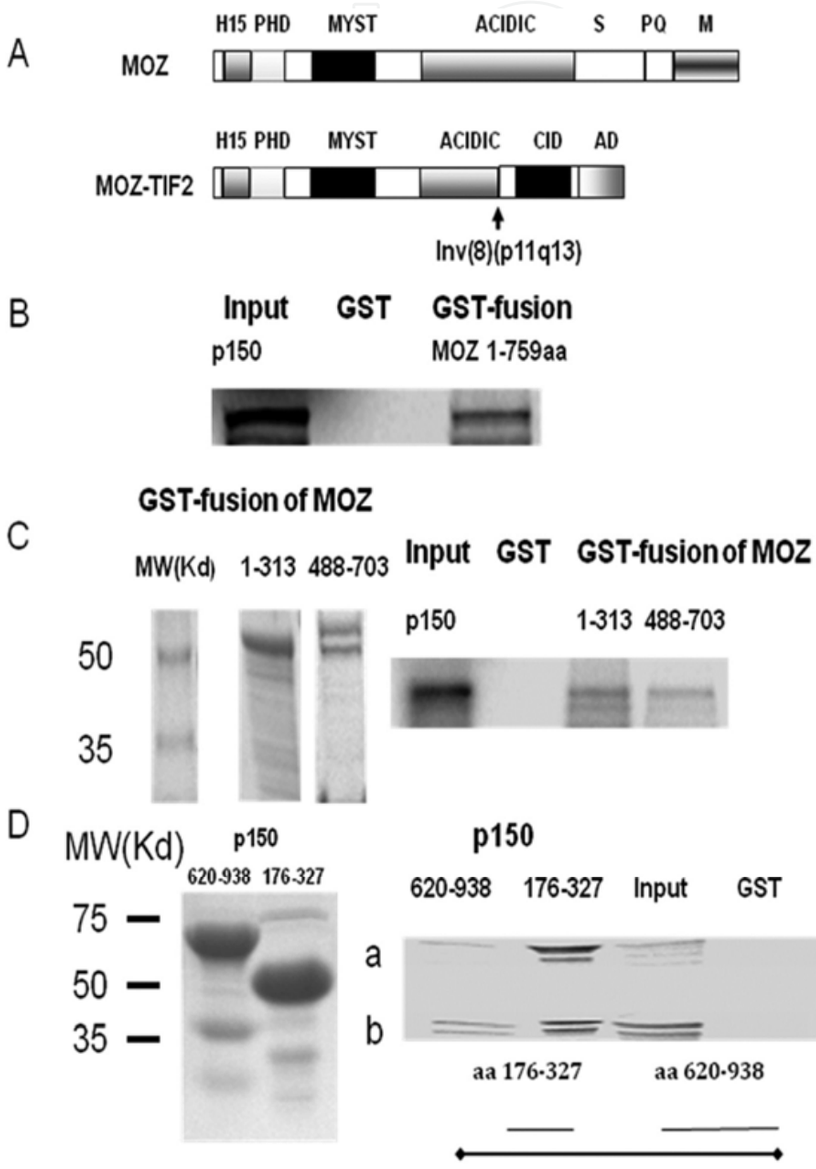

Fig. 3. The interaction between MOZ fragments and CAF-1A (p150). GST-tagged MOZ fragments were expressed and purified with glutathione Sepharose 4B as described in Materials and Methods. [35S]-methionine labeled p150 protein was produced from a T7-driven pET-30 plasmid with an *in vitro* translation system. A, binding assay was conducted with [35S]-methionine labeled p150 and the GST-tagged MOZ fragments. The input lane is 10% of the [35S] methionine p150 protein added to the binding assay. A, schematic structure

of MOZ and MOZ-TIF2. B, interaction between p150 and the MOZ fragment from amino acids 1 to 759 using the binding assay as described in the Materials and Methods. C, left panel, SDS-PAGE of the purified GST-MOZ-1/313 and GST-MOZ-488/703 peptides to demonstrate that the peptides were of the expected molecular weights; right panel, as described in Materials and Methods [^{35}S]-methionine labeled p150 synthesized in a cell-free translation system was incubated *in vitro* with equivalent amounts of GST fusions with MOZ-1/313 or MOZ-488/703, the resulting complexes isolated by GST-pull down assay, and the amount of [^{35}S]-methionine labeled p150 detected by radioautography following SDS-PAGE. D, left panel, SDS-PAGE of the purified GST-p150-176/327 and GST-p150-620/938 fusion peptides; right panel, GST pulldown assays as described in C with [^{35}S]-methionine labeled MOZ-1/313 (a) and MOZ-488/703(b) peptides. The bottom line indicates the full length p150 protein.

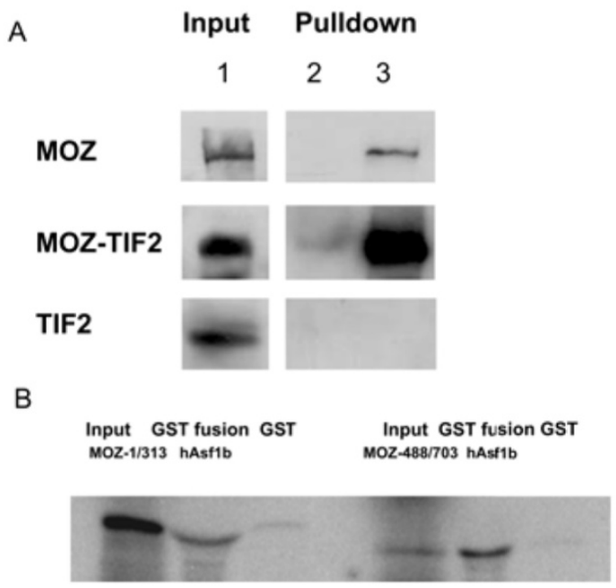

Fig. 4. ASF1B interacts with MOZ and MOZ-TIF2. **Panel A**. HEK293 cells were transfected with EGFP-MOZ, EGFP-MOZ-TIF2, and EGFP-TIF2 as detailed in the Materials and Methods. At 48 hours after transfection cell lysates were incubated with S–tagged ASF1B absorbed to S-tag agarose beads and after extensive washing the proteins bound to ASF1B were analyzed by SDS-PAGE with subsequent western blot analysis with anti-GFP antibody. Lane 1, 10% of input; lane 2, S-tag protein alone; lane 3, S-tagged ASF1B. **Panel B**. GST pull down assays were performed as detailed above incubating GST- ASF1B with [^{35}S]-methionine labeled MOZ-1/313 or MOZ-488/703 peptides synthesized in a cell-free translation system as described in the Material and Methods.

3.4 Confirmation of ASF1B as an interacting protein of MOZ and MOZ-TIF2

The yeast two-hybrid system also revealed a cDNA encoding another protein, ASF1B, which interacted with the MOZ-1/759 fragment. To verify the interaction between MOZ

and ASF1B and to examine if the MOZ-TIF2 fusion protein also interacts with ASF1B, we conducted pull down assays and examined co-localization of proteins similar to the studies with CAF-1A. A S-tag fusion cDNA with ASF1B was created in the pET-30c vector and the fusion protein was labeled with [^{35}S]methionine by an in vitro transcription/translation system. The expressed fusion protein was purified with S-tag agarose beads and incubated with cell lysates containing expressed EGFP fusions of MOZ, MOZ-TIF2 and TIF2. Subsequently, EGFP proteins that interacted with ASF1B were identified by western blot analysis with an anti-EGFP antibody (Figure 4A). Both EGFP-MOZ and EGFP-MOZ-TIF2 could be demonstrated to interact with ASF1B. MOZ-TIF2 appeared to interact more strongly with the percentage of EGFP fusion protein bound to ASF1B approximately 240% over the input for MOZ-TIF2 and 70% for MOZ, respectively. TIF2 showed no binding to ASF1B. To further identify the ASF1B binding domain in MOZ, the GST-tagged ASF1B was incubated with [^{35}S]methionine labeled MOZ-1/313 and MOZ-488/703 (Figure 4B). The MOZ-488/703 fragment showed stronger binding to ASF1B than MOZ-1/313. The percentage of ASF1B bound to the MOZ-1/313 fragment represented about 25% of the input while the percentage of ASF1B bound to the MOZ-488/703 fragment was 150% of the input.

3.5 The co-localization of MOZ and MOZ-TIF2 with CAF-1A and ASF1B

To further verify the interaction of MOZ with CAF-1A, we first examined by indirect immunohistochemistry the localization of endogenous MOZ and CAF-1A in Hela cells to determine if the subcellular distribution was similar by confocal immunofluorescence microscopy (Figure 5A). In Hela cells both MOZ and CAF-1A were predominately localized in interphase nuclei (Figure 5A-a). As the chromatin condensed in metaphase MOZ distributed dominantly in cytoplasm and disassociated from the spindle-chromosome in some cells (Figure 5A-b and 5A-c). CAF-1A was observed either to disassociate from (Figure 5A-b) or bind to spindle-chromosomes (Figure 5A-c). However, cytoplasmic co-localization of MOZ and CAF-1A was still seen as detected by the persistence of yellow by confocal microscopy. In anaphase, with paired chromosome separation, CAF-1A was still bound to the spindle-chromosome but MOZ was fully dissociated (Figure 5A-d) but with persistent co-localization of both in the cytoplasm. To determine if the MOZ-TIF2 fusion protein has similar localization as MOZ and co-localized with CAF-1A, HEK293 cells were transfected with EGFP-MOZ or EGFP-MOZ-TIF2 and DsRed2-CAF-1A (Figure 5B). Both EGFP-MOZ and EGFP-MOZ-TIF2 showed a predominantly nuclear localization in HEK293 cells in interphase. However, the, EGFP-MOZ-TIF2 fusion protein appeared in larger aggregates compared to the more homogenously distributed MOZ. In the merged image the MOZ co-localization with CAF-1A appeared stronger than the MOZ-TIF2-CAF-1A co-localization (Figure 5B, top panel, merge). To examine the binding of MOZ, MOZ-TIF2, and CAF-1A to the interphase chromatin we conducted pre-extraction with Triton-X100 in EGFP-MOZ and EGFP-MOZ-TIF2 transfected HEK293 cells (Figure 5C). In the interphase, all three proteins, EGFP-MOZ, EGFP-MOZ-TIF2, and CAF-1A showed resistance to pre-extraction and the co-localization with DAPI-stained DNA. Similarly, the co-localization of EGFP-MOZ-TIF2 with ASF1B was shown in transfected HEK293 cells (Figure 6A). Interestingly, EGFP-MOZ-TIF2 exhibited stronger co-localization with DsRed2-ASF1B than EGFP-MOZ in pre-extracted HEK293 cells (Figure 6B, merge).

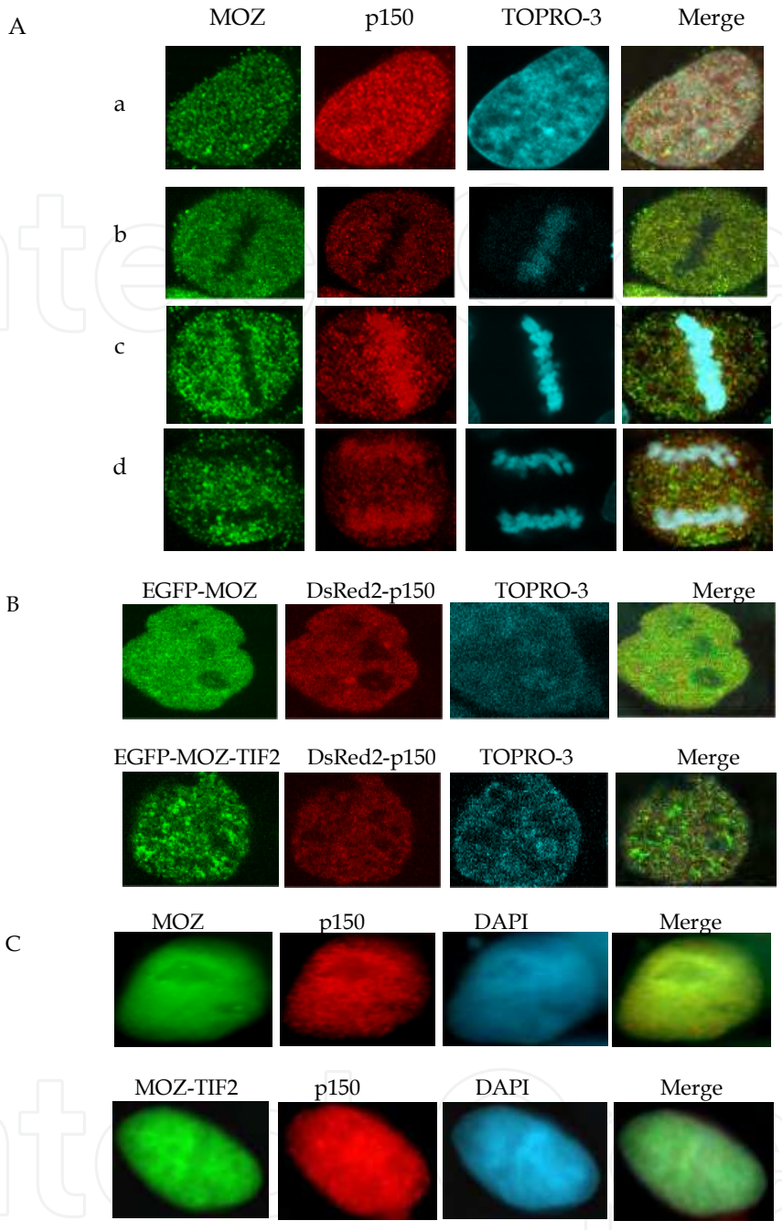

Fig. 5. Subcellular localization of MOZ, MOZ-TIF2, CAF-1A **(**p150). **A**. Indirect immunofluorescence of MOZ (green) and p150 (red) in HeLa cells at interphase and metaphase observed by confocal microscopy with the nuclei stained with Topro-3. **B**. Confocal microscope images were obtained of HEK293 cells co-transfected with EGFP-MOZ and DsRed2-p150 or EGFP-MOZ-TIF2 and DsRed2-p150 as detailed in the Materials and Methods and nuclei stained with Topro-3. **C**. HEK293 cells transfected with EGFP-MOZ (green) and EGFP-MOZ-TIF2 (green) and stained with anti-p150 antibody after pre-extraction with Triton-X100. The fluorescent images were obtained at x100 with a Zeiss fluorescent microscope.

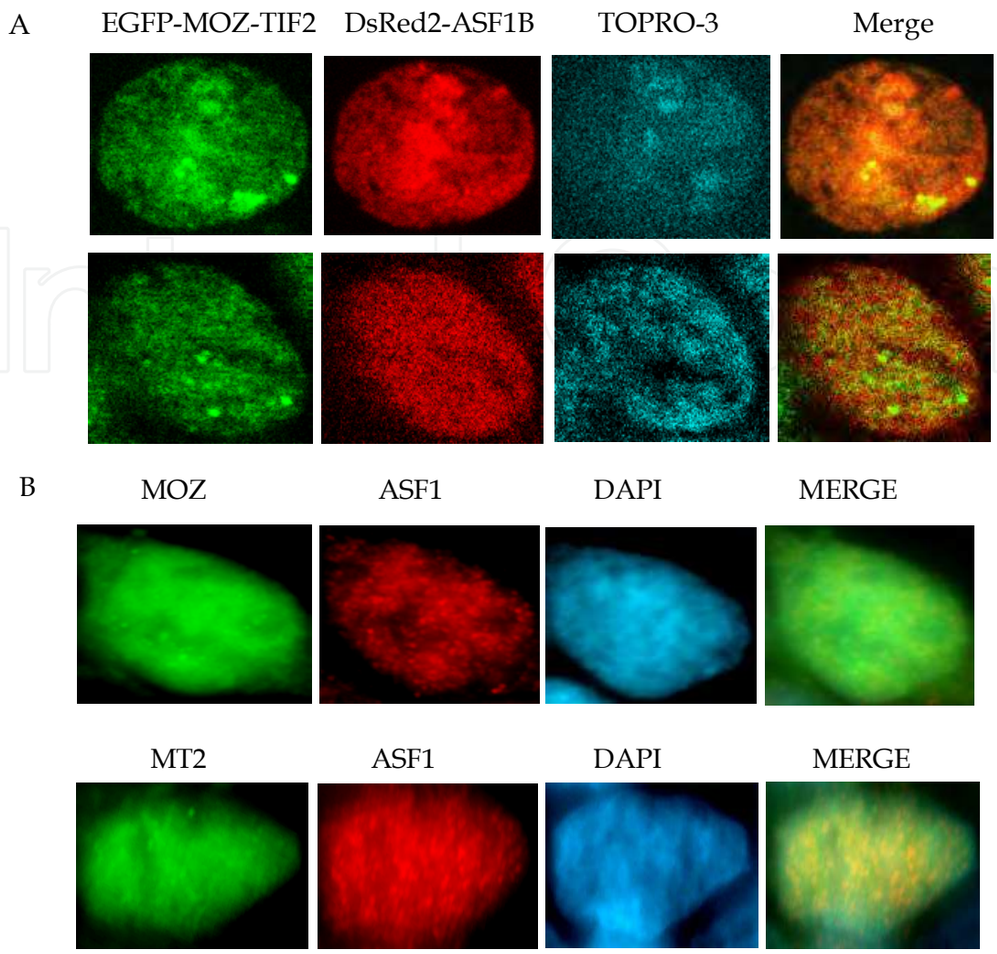

Fig. 6. **A**. Confocal microscope images were obtained of HEK293 cells co-transfected with EGFP-MOZ-TIF2 and DsRed2-ASF1B. The nuclei were stained with Topro-3. **B**. HEK293 cells were transfected with EGFP-MOZ or EGFP-MOZ-TIF2. 48 hours later, cells were pre-extracted, fixed, and immune-stained with anti-ASF1B antibody. Fluorescent images were photographed at x100 with a Zeiss fluorescent microscope.

3.6 Altered gene expression profile in U937 cells stably transfected with MOZ-TIF2

CAF-1 and ASF1, as histone chaperon proteins are essential in maintaining the nucleosome structure after DNA replica and in DNA repair. In yeast, CAF-1 and ASF1 are regulators of global gene expression (Zabaronick and Tyler, 2005). However, if MOZ and MOZ-TIF2, as proteins that associate with CAF-1 and ASF1, affect global gene expression is not known. We established stable transfection clones from U937 cells with forced expression of MOZ and MOZ-TIF2 and analyzed global gene expression of these cell clones. Compared to the expression profile of control cells stably transfected with pcDNA3 vector alone, MT2 caused a > 2-fold change in expression with 181 genes increasing and 106 genes decreasing expression (p = 0.01). Over expression of wild type MOZ also altered gene expression (>2-fold increase in 132 genes and >2-fold decrease in 88 genes, p=0.01). In addition, a differential gene expression signature was seen between MOZ and MOZ-TIF2 in a Venn

diagram analysis (Figure 7). The signature-expressed genes are 189 with pcDNA3, 84 with MOZ, and 427 with MOZ-TIF2, respectively. Further pairwise analysis of differential expression of genes between MOZ and MOZ-TIF2 indicated that there 28 genes increasing over 2 fold (Table 1) and 34 genes decreasing over 2 fold (Table 2) in MOZ-TIF2 compared with that in MOZ. The altered genes between MOZ and MOZ-TIF2 are involved in multiple cell functions such as signal transduction, cell response to stimulus, cell cycle, chromosome structure, development, and tumor progression.

Ratio	p-value	Gene Name
6.41	0.002777	Transcribed locus, weakly similar to XP_537423.2 PREDICTED: similar to LINE-1 reverse transcriptase homolog [Canis familiaris
5.78	0.001076	Malic enzyme 3, NADP(+)-dependent, mitochondrial
4.8	0.042772	Testis derived transcript (3 LIM domains)
4.01	0.021676	Bone morphogenetic protein 1
3.71	0.031657	Interleukin 8 receptor, beta
3.63	0.012968	NADH dehydrogenase (ubiquinone) 1 beta subcomplex, 6, 17kDa
3.09	0.042154	calreticulin
2.73	0.047444	Actin binding LIM protein 1
2.55	0.040271	Ribosome binding protein 1 homolog 180kDa (dog)
2.43	0.016348	vesicle amine transport protein 1 homolog (T. californica)
2.41	0.004052	Calreticulin
2.39	0.039279	histone cluster 1, H2bi
2.37	0.039548	insulin-like growth factor binding protein 2, 36kDa
2.36	0.012714	Inversin
2.36	0.048093	PTK2B protein tyrosine kinase 2 beta
2.29	0.010907	RAP1 interacting factor homolog (yeast)
2.22	0.00445	CD160 molecule
2.13	0.042832	Carnitine palmitoyltransferase 1B (muscle)
2.13	0.010751	PCTAIRE protein kinase 1
2.12	0.006671	Neutrophil cytosolic factor 4, 40kDa
2.11	0.039481	neurogranin (protein kinase C substrate, RC3)
2.1	0.036043	Tyrosine 3-monooxygenase/tryptophan 5-monooxygenase activation protein, epsilon polypeptide
2.09	0.002837	Mediator complex subunit 21
2.06	0.008281	Insulin-like growth factor binding protein 2, 36kDa
2.04	0.032872	acylphosphatase 2, muscle type
2.03	0.006805	FK506 binding protein 1A, 12kDa
2.02	0.006539	Neurochondrin
2	0.001062	Syntaxin 5

Table 1. Up-regulated genes in MOZ-TIF2 vs MOZ.

Ratio	p-value	Gene Name
14.58	0.034066	Fibroblast growth factor receptor 2
10.51	0.048971	Transcribed locus
5.7	0.020122	Spectrin, beta, non-erythrocytic 1
5.3	0.007972	Sulfotransferase (Sulfokinase) like gene, a putative GS2 like gene
5.17	0.005226	Defensin, beta 1
3.92	0.00956	chorionic somatomammotropin hormone-like 1
3.68	0.002866	elongation factor, RNA polymerase II, 2
3.64	0.04087	RAP2A, member of RAS oncogene family
3.57	0.040904	CD2 molecule
3.57	0.039775	Met proto-oncogene (hepatocyte growth factor receptor)
3.34	6.34E-05	Adipose differentiation-related protein
2.99	0.049188	ATPase, Ca++ transporting, plasma membrane 4
2.61	0.013043	X-ray repair complementing defective repair in Chinese hamster cells 2
2.49	0.002229	regulatory solute carrier protein, family 1, member 1
2.47	0.018837	CMP-N-acetylneuraminate monooxygenase) pseudogene
2.45	0.049139	Angiogenic factor with G patch and FHA domains 1
2.45	0.026164	SCY1-like 3 (S. cerevisiae)
2.36	0.003507	spermidine/spermine N1-acetyltransferase 1
2.34	0.046867	ATPase, class VI, type 11A
2.27	0.027531	ecotropic viral integration site 2A
2.22	0.045457	Ubiquitin specific peptidase like 1
2.21	0.035349	Cyclin-dependent kinase 6
2.17	0.000434	CDC14 cell division cycle 14 homolog B (S. cerevisiae)
2.17	0.032088	Kruppel-like factor 10
2.17	0.049619	Starch binding domain 1
2.16	0.023854	Homeodomain interacting protein kinase 3
2.15	0.030337	Ectodermal-neural cortex (with BTB-like domain)
2.14	0.010869	Angiogenic factor with G patch and FHA domains 1
2.12	0.049079	Reversion-inducing-cysteine-rich protein with kazal motifs
2.11	0.042149	suppressor of Ty 3 homolog (S. cerevisiae)
2.08	0.037371	Nuclear receptor subfamily 1, group D, member 2
2.08	0.022954	cytochrome P450, family 1, subfamily A, polypeptide 1
2.06	0.004142	Peroxisomal biogenesis factor 5
2.06	0.033184	Fem-1 homolog c (C. elegans)

Table 2. Down-regulated genes in MOZ-TIF2 vs MOZ.

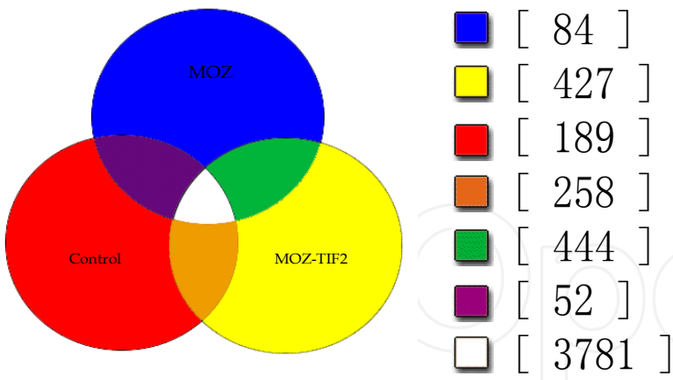

Fig. 7. The Venn diagram of signature gene expression among pcDNA3, MOZ, and MOZ-TIF2. The positive expressed genes were picked up as described in Materials and Methods. The number in brackets indicates the signature genes.

4. Discussion

In order to gain understanding of the function of the MOZ-TIF2 fusion protein we used the yeast two-hybrid system to screen a human bone marrow cDNA library and identified two proteins, CAF-1A and ASF1B, that interacted with the MOZ partner of MOZ-TIF2. The CAF-1A is the largest subunit of CAF-1 which is responsible for bringing histones H3 and H4 to newly synthesized DNA to constitute a nucleosome during DNA replication and DNA repair (Moggs et al., 2000; Shibahara and Stillman, 1999; Smith and Stillman, 1989). CAF-1 controls S-phase progression in euchromatic DNA replication (Klapholz et al., 2009). During chromatin assembly CAF-1 is localized at the replication loci through the association with the proliferation cell nuclear antigen (PCNA), interacting with the N-terminal PCNA binding motif in the CAF-1A. CAF-1 has also been shown to have a role in transcription regulation and epigenetic control of gene expression by interacting with methyl-CpG binding protein and by contributing non-methylation dependent gene silencing (Reese et al., 2003; Sarraf and Stancheva, 2004; Tchenio et al., 2001). A dominant-negative mutant of CAF-1A arrests cell cycle in S-phase (Ye et al., 2003). The loss of CAF-1 is lethal in human cells and increases the sensitivity of cells to UV and other DNA damaging reagents (Game and Kaufman, 1999; Nabatiyan and Krude, 2004). In addition, CAF-1 has been suggested as a clinical marker to distinguish quiescent from proliferating cells (Polo et al., 2004). ASF1B, the other MOZ-TIF2 interacting protein identified, is one of two human ASF1 proteins and participates in chromatin assembly by interacting with the p60 unit of CAF-1 (Mello et al., 2002). The function of ASF1 overlaps with CAF-1 but contributes mainly to chromatin-mediated gene silencing (Meijsing and Ehrenhofer-Murray, 2001; Mello et al., 2002; Osada et al., 2001). In the process of nucleosome formation during DNA replication, ASF1 synergizes functionally with CAF-1 by binding histone H3/H4 and delivers histone H3 and H4 dimers to CAF-1 (Tyler et al., 1999; Tyler et al., 2001). As with CAF-1 mutations, mutations in ASF1 raise the sensitivity of cells to DNA damage (Daganzo et al., 2003; Emili et al., 2001; Le et al., 1997). In yeast, the absence of ASF1 leads to enhanced genetic instability and sister chromatid exchange (Prado et al., 2004). Recent study revealed that the expression of ASF1B, like CAF-1A, was proliferation-dependent (Corpet et al., 2011). Both CAF-1 and ASF1 are

important in maintaining genetic stability and hence mutations or aberrant expression in either may contribute to carcinogenesis.

Our initial results demonstrated that the MOZ portion of the MOZ-TIF2 fusion protein interacted with the human CAF-1A and ASF1B. These associations are consistent with previous findings that a MYST family member in yeast, SAS (something about silencing) protein, interacts with Cac1, a yeast homologue of human CAF-1A, and yeast ASF1 and that the interaction contributed to the silencing of the ribosomal DNA locus (Meijsing and Ehrenhofer-Murray, 2001). However, in our experiments with the yeast two-hybrid system, the association between the MOZ-1/759 fragment and CAF-1A was stronger than the interaction of the MOZ-1/759 fragment and ASF1B. The clones of MOZ-1/759 and CAF-1A grew in both –His and –Ade selection media while the clones of MOZ-1/759 and ASF1B grew only in the –His medium. These results suggest that the intensity of interaction of the MOZ fragment with each chaperone is different and the interactions may involve different domains of MOZ. With the GST pull-down assays, we were able to verify the physical interactions using purified proteins and to begin probing the regions of MOZ involved in the interactions. Our results demonstrated that CAF-1A bound primarily to the N-terminus of MOZ (MOZ-1/313) while ASF1B bound to the domain containing C2HC motif and acetyl-CoA binding region (MOZ-488/703). To exclude possible indirect interactions caused by using a mammalian transcription/ translation system, the pull-down assay was also conducted using an E. coli translation system (EcoPro™ T7 System, EMD Biosciences, Novagen, San Diego, CA) with the same interactions being seen again (data not shown). The binding of CAF-1A and ASF1B to two distinct regions within the MOZ fragment involved in the MOZ-TIF2 fusion protein suggests that MOZ-TIF2 positively influences participation in chromatin assembly.

The experiments reported here also begin to shed some light on aberrant function of the MOZ-TIF2 fusion protein by comparing semi-quantatively the strength of association of CAF-1A and ASF1B with MOZ and MOZ-TIF2. In the co-immunopreciptiation and S-tagged pull down experiments, CAF-1A appeared to interact more strongly with MOZ than MOZ-TIF2. These observations were confirmed by the increased co-localization seen in confocal microscopy of the co-transfected cells at interphase. The converse was seen in the interactions of ASF1B with an apparent greater intensity of interaction of ASF1B with MOZ-TIF2 than MOZ alone. Again, this interaction was confirmed in pre-extracted HEK293 cells. It seems that MOZ-TIF2 fusion protein changed the binding priorities of MOZ. These differences may occur because of the necessity of appropriate folding or other higher order structural changes in the full-length MOZ, which are obviated in the fusion protein. In addition, we noticed that the localization of MOZ and CAF-1A was altered in mitotic cells, suggesting that the function of interactions in chromatin assembly and modification depend on cell division cycle. Previously, CAF-1 has been observed to disassociate from chromosomes during the M phase and to be inactivated in mitosis (Marheineke and Krude, 1998). However, we have seen the binding of CAF-1A to the spindle-like chromosome during the metaphase and anaphase in immune-stained Hela cells. It is not clear if the altered association of CAF-1A with chromosome indicates a physiological process during the mitosis or is the artificial results either of fixation and stain process or the limitation of the antibody. A further investigation is necessary to determine the dynamic change of the association.

Using stably transfected U937 cells, we were able to find MOZ-TIF2-correlated changes in the global expression profile of genes and identify a signature-expression profile for MOZ-TIF2. However, as MOZ and TIF2 function as transcription co-factors and as CAF-1 and ASF1 are regulators of global transcription the altered gene expression by MOZ-TIF2 cannot be ascribed to the interaction of MOZ-TIF2 with CAF-1A and ASF1B alone. Interestingly, inspite of 427 expressed signature genes of MOZ-TIF2, only 62 genes were found with over two-fold significant change between MOZ-TIF2 and MOZ, suggesting that differences in expression level between MOZ and MOZ-TIF2 of most most signature genes signature genes could be relatively small.

We are currently examining the hypothesis that the association of MOZ-TIF2 with chromatin assembly factors affects the nucleosome structure and/or histone modification such that histone acetylation status would contribute to leukemogenesis. This hypothesis assumes that the MOZ-TIF2 fusion protein may alter constitution of the chromatin assembly factor complex and then change global gene expression. A possible target for this type of altered function would be that the fusion protein could alter the recruitment of CBP to the complex via LXXLL motifs in TIF2 portion (Voegel et al., 1998; Yin et al., 2007).

5. Conclusions

We demonstrate that both MOZ and MOZ-TIF2 interacts with ASF1B via its MYST domain and interacts with CAF-1A via its zinc finger domain. MOZ and MOZ–TIF2 co-localize with CAF-1A and ASF1B in interphase nuclei. MOZ-TIF2, compared to MOZ, preferentially binds to ASF1B rather than to CAF-1A. MOZ-TIF2 interferes with the function of wild type MOZ and alters global gene expression in U937 cells.

6. References

Aikawa, Y., Katsumoto, T., Zhang, P., Shima, H., Shino, M., Terui, K., Ito, E., Ohno, H., Stanley, E. R., Singh, H., *et al.* (2010). PU.1-mediated upregulation of CSF1R is crucial for leukemia stem cell potential induced by MOZ-TIF2. Nat Med *16*, 580-585, 581p following 585.

Bristow, C. A., and Shore, P. (2003). Transcriptional regulation of the human MIP-1alpha promoter by RUNX1 and MOZ. Nucleic Acids Res *31*, 2735-2744.

Champagne, N., Bertos, N. R., Pelletier, N., Wang, A. H., Vezmar, M., Yang, Y., Heng, H. H., and Yang, X. J. (1999). Identification of a human histone acetyltransferase related to monocytic leukemia zinc finger protein. J Biol Chem *274*, 28528-28536.

Champagne, N., Pelletier, N., and Yang, X. J. (2001). The monocytic leukemia zinc finger protein MOZ is a histone acetyltransferase. Oncogene *20*, 404-409.

Corpet, A., De Koning, L., Toedling, J., Savignoni, A., Berger, F., Lemaitre, C., O'Sullivan, R. J., Karlseder, J., Barillot, E., Asselain, B., *et al.* (2011). Asf1b, the necessary Asf1 isoform for proliferation, is predictive of outcome in breast cancer. Embo J *30*, 480-493.

Daganzo, S. M., Erzberger, J. P., Lam, W. M., Skordalakes, E., Zhang, R., Franco, A. A., Brill, S. J., Adams, P. D., Berger, J. M., and Kaufman, P. D. (2003). Structure and function of the conserved core of histone deposition protein Asf1. Curr Biol *13*, 2148-2158.

Deguchi, K., Ayton, P. M., Carapeti, M., Kutok, J. L., Snyder, C. S., Williams, I. R., Cross, N. C., Glass, C. K., Cleary, M. L., and Gilliland, D. G. (2003). MOZ-TIF2-induced acute myeloid leukemia requires the MOZ nucleosome binding motif and TIF2-mediated recruitment of CBP. Cancer Cell *3*, 259-271.

Emili, A., Schieltz, D. M., Yates, J. R., 3rd, and Hartwell, L. H. (2001). Dynamic interaction of DNA damage checkpoint protein Rad53 with chromatin assembly factor Asf1. Mol Cell *7*, 13-20.

Esteyries, S., Perot, C., Adelaide, J., Imbert, M., Lagarde, A., Pautas, C., Olschwang, S., Birnbaum, D., Chaffanet, M., and Mozziconacci, M. J. (2008). NCOA3, a new fusion partner for MOZ/MYST3 in M5 acute myeloid leukemia. Leukemia *22*, 663-665.

Game, J. C., and Kaufman, P. D. (1999). Role of Saccharomyces cerevisiae chromatin assembly factor-I in repair of ultraviolet radiation damage in vivo. Genetics *151*, 485-497.

Huntly, B. J., Shigematsu, H., Deguchi, K., Lee, B. H., Mizuno, S., Duclos, N., Rowan, R., Amaral, S., Curley, D., Williams, I. R., *et al.* (2004). MOZ-TIF2, but not BCR-ABL, confers properties of leukemic stem cells to committed murine hematopoietic progenitors. Cancer Cell *6*, 587-596.

James, P., Halladay, J., and Craig, E. A. (1996). Genomic libraries and a host strain designed for highly efficient two-hybrid selection in yeast. Genetics *144*, 1425-1436.

Katsumoto, T., Aikawa, Y., Iwama, A., Ueda, S., Ichikawa, H., Ochiya, T., and Kitabayashi, I. (2006). MOZ is essential for maintenance of hematopoietic stem cells. Genes Dev *20*, 1321-1330.

Katsumoto, T., Yoshida, N., and Kitabayashi, I. (2008). Roles of the histone acetyltransferase monocytic leukemia zinc finger protein in normal and malignant hematopoiesis. Cancer Sci *99*, 1523-1527.

Kitabayashi, I., Aikawa, Y., Nguyen, L. A., Yokoyama, A., and Ohki, M. (2001). Activation of AML1-mediated transcription by MOZ and inhibition by the MOZ-CBP fusion protein. Embo J *20*, 7184-7196.

Klapholz, B., Dietrich, B. H., Schaffner, C., Heredia, F., Quivy, J. P., Almouzni, G., and Dostatni, N. (2009). CAF-1 is required for efficient replication of euchromatic DNA in Drosophila larval endocycling cells. Chromosoma *118*, 235-248.

Le, S., Davis, C., Konopka, J. B., and Sternglanz, R. (1997). Two new S-phase-specific genes from Saccharomyces cerevisiae. Yeast *13*, 1029-1042.

Liang, J., Prouty, L., Williams, B. J., Dayton, M. A., and Blanchard, K. L. (1998). Acute mixed lineage leukemia with an inv(8)(p11q13) resulting in fusion of the genes for MOZ and TIF2. Blood *92*, 2118-2122.

Marheineke, K., and Krude, T. (1998). Nucleosome assembly activity and intracellular localization of human CAF-1 changes during the cell division cycle. J Biol Chem *273*, 15279-15286.

Meijsing, S. H., and Ehrenhofer-Murray, A. E. (2001). The silencing complex SAS-I links histone acetylation to the assembly of repressed chromatin by CAF-I and Asf1 in Saccharomyces cerevisiae. Genes Dev *15*, 3169-3182.

Mello, J. A., Sillje, H. H., Roche, D. M., Kirschner, D. B., Nigg, E. A., and Almouzni, G. (2002). Human Asf1 and CAF-1 interact and synergize in a repair-coupled nucleosome assembly pathway. EMBO Rep *3*, 329-334.

Moggs, J. G., Grandi, P., Quivy, J. P., Jonsson, Z. O., Hubscher, U., Becker, P. B., and Almouzni, G. (2000). A CAF-1-PCNA-mediated chromatin assembly pathway triggered by sensing DNA damage. Mol Cell Biol *20*, 1206-1218.

Nabatiyan, A., and Krude, T. (2004). Silencing of chromatin assembly factor 1 in human cells leads to cell death and loss of chromatin assembly during DNA synthesis. Mol Cell Biol *24*, 2853-2862.

Osada, S., Sutton, A., Muster, N., Brown, C. E., Yates, J. R., 3rd, Sternglanz, R., and Workman, J. L. (2001). The yeast SAS (something about silencing) protein complex contains a MYST-type putative acetyltransferase and functions with chromatin assembly factor ASF1. Genes Dev *15*, 3155-3168.

Perez-Campo, F. M., Borrow, J., Kouskoff, V., and Lacaud, G. (2009). The histone acetyl transferase activity of monocytic leukemia zinc finger is critical for the proliferation of hematopoietic precursors. Blood *113*, 4866-4874.

Polo, S. E., Theocharis, S. E., Klijanienko, J., Savignoni, A., Asselain, B., Vielh, P., and Almouzni, G. (2004). Chromatin assembly factor-1, a marker of clinical value to distinguish quiescent from proliferating cells. Cancer Res *64*, 2371-2381.

Prado, F., Cortes-Ledesma, F., and Aguilera, A. (2004). The absence of the yeast chromatin assembly factor Asf1 increases genomic instability and sister chromatid exchange. EMBO Rep *5*, 497-502.

Reese, B. E., Bachman, K. E., Baylin, S. B., and Rountree, M. R. (2003). The methyl-CpG binding protein MBD1 interacts with the p150 subunit of chromatin assembly factor 1. Mol Cell Biol *23*, 3226-3236.

Sarraf, S. A., and Stancheva, I. (2004). Methyl-CpG binding protein MBD1 couples histone H3 methylation at lysine 9 by SETDB1 to DNA replication and chromatin assembly. Mol Cell *15*, 595-605.

Shibahara, K., and Stillman, B. (1999). Replication-dependent marking of DNA by PCNA facilitates CAF-1-coupled inheritance of chromatin. Cell *96*, 575-585.

Smith, S., and Stillman, B. (1989). Purification and characterization of CAF-I, a human cell factor required for chromatin assembly during DNA replication in vitro. Cell *58*, 15-25.

Tchenio, T., Casella, J. F., and Heidmann, T. (2001). A truncated form of the human CAF-1 p150 subunit impairs the maintenance of transcriptional gene silencing in mammalian cells. Mol Cell Biol *21*, 1953-1961.

Troke, P. J., Kindle, K. B., Collins, H. M., and Heery, D. M. (2006). MOZ fusion proteins in acute myeloid leukaemia. Biochem Soc Symp, 23-39.

Tyler, J. K., Adams, C. R., Chen, S. R., Kobayashi, R., Kamakaka, R. T., and Kadonaga, J. T. (1999). The RCAF complex mediates chromatin assembly during DNA replication and repair. Nature *402*, 555-560.

Tyler, J. K., Collins, K. A., Prasad-Sinha, J., Amiott, E., Bulger, M., Harte, P. J., Kobayashi, R., and Kadonaga, J. T. (2001). Interaction between the Drosophila CAF-1 and ASF1 chromatin assembly factors. Mol Cell Biol *21*, 6574-6584.

Voegel, J. J., Heine, M. J., Tini, M., Vivat, V., Chambon, P., and Gronemeyer, H. (1998). The coactivator TIF2 contains three nuclear receptor-binding motifs and mediates transactivation through CBP binding-dependent and -independent pathways. Embo J *17*, 507-519.

Ye, X., Franco, A. A., Santos, H., Nelson, D. M., Kaufman, P. D., and Adams, P. D. (2003). Defective S phase chromatin assembly causes DNA damage, activation of the S phase checkpoint, and S phase arrest. Mol Cell *11*, 341-351.

Yin, H., Glass, J., and Blanchard, K. L. (2007). MOZ-TIF2 repression of nuclear receptor-mediated transcription requires multiple domains in MOZ and in the CID domain of TIF2. Mol Cancer *6*, 51.

Zabaronick, S. R., and Tyler, J. K. (2005). The histone chaperone anti-silencing function 1 is a global regulator of transcription independent of passage through S phase. Mol Cell Biol *25*, 652-660.

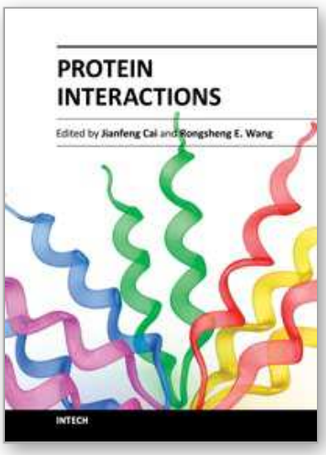

Protein Interactions

Edited by Dr. Jianfeng Cai

ISBN 978-953-51-0244-1
Hard cover, 464 pages
Publisher InTech
Published online 16, March, 2012
Published in print edition March, 2012

Protein interactions, which include interactions between proteins and other biomolecules, are essential to all aspects of biological processes, such as cell growth, differentiation, and apoptosis. Therefore, investigation and modulation of protein interactions are of significance as it not only reveals the mechanism governing cellular activity, but also leads to potential agents for the treatment of various diseases. The objective of this book is to highlight some of the latest approaches in the study of protein interactions, including modulation of protein interactions, development of analytical techniques, etc. Collectively they demonstrate the importance and the possibility for the further investigation and modulation of protein interactions as technology is evolving.

InTech Europe
University Campus STeP Ri
Slavka Krautzeka 83/A
51000 Rijeka, Croatia
Phone: +385 (51) 770 447
Fax: +385 (51) 686 166
www.intechopen.com

InTech China
Unit 405, Office Block, Hotel Equatorial Shanghai
No.65, Yan An Road (West), Shanghai, 200040, China
中国上海市延安西路65号上海国际贵都大饭店办公楼405单元
Phone: +86-21-62489820
Fax: +86-21-62489821

IntechOpen